Stability of Vacancy Clusters in Metals I: Energy Calculations for Pure Metals

S.J. Zinkle, L.E. Seitzman, W.G. Wolfer

June 1986

UWFDM-692

FUSION TECHNOLOGY INSTITUTE

UNIVERSITY OF WISCONSIN

MADISON WISCONSIN

Stability of Vacancy Clusters in Metals I: Energy Calculations for Pure Metals

S.J. Zinkle, L.E. Seitzman, W.G. Wolfer

Fusion Technology Institute
University of Wisconsin
1500 Engineering Drive
Madison, WI 53706

http://fti.neep.wisc.edu

June 1986

UWFDM-692

STABILITY OF VACANCY CLUSTERS IN METALS I

ENERGY CALCULATIONS FOR PURE METALS

S.J. Zinkle[1], L.E. Seitzman and W.G. Wolfer[2]

University of Wisconsin
Fusion Technology Institute
1500 Johnson Drive
Madison, WI 53706-1687

August 1986

[1] Present Address: Metals and Ceramics Division, Oak Ridge National Laboratory, Oak Ridge, Tennessee USA 37831

[2] Present Address: Sandia National Laboratory, Livermore, California 94550

UWFDM-692

1. Introduction

A supersaturation of vacancies can be created in a metal by energetic particle irradiation, quenching, or mechanical deformation. At temperatures where the vacancy is mobile (generally $\gtrsim 0.3\ T_M$, where T_M is the melting temperature) these vacancies can migrate and coalesce to form microscopic clusters. The final geometry of the resultant vacancy clusters can have a significant impact on the macroscopic behavior of the metal. The formation of planar vacancy clusters such as dislocation loops tends to strengthen the metal. On the other hand, formation of three-dimensional voids can produce a significant amount of swelling.

Various authors have previously calculated the relative stability of the different vacancy cluster geometries that may occur in metals by utilizing established elastic continuum expressions (Sigler and Kuhlmann-Wilsdorf 1966, Cotterill 1966, Buswell 1970). Some differences exist between these authors' predictions of the most stable vacancy cluster geometry for different representative metals. These discrepancies are mainly caused by the use of different experimental data (or estimates of data) for the materials parameters used in the continuum calculations, in particular surface energy data. Comparison of the calculations with experimental results has also generally revealed important disagreements with regard to the most stable vacancy cluster morphology.

The purpose of the present paper is to re-analyze the stability of various vacancy cluster geometries in a variety of metals using the appropriate current material properties data. Calculations are performed for six representative fcc metals (gold, silver, aluminum, copper, nickel, stainless steel) and two bcc metals (α-iron and molybdenum). These metals were chosen because

their properties and vacancy cluster geometries have been well-studied. It is well established that the observed vacancy cluster morphology in a given metal is strongly influenced by the presence of impurities. In particular, introduction of gaseous impurity concentrations of as little as 10 appm may result in a completely different cluster geometry compared to the pure metal case (see Section 4.2). A model is presented in the companion paper (Zinkle, Wolfer, Kulcinski and Seitzman 1985, to be referred to as Part II) for determining the effects of oxygen and helium on vacancy cluster energies.

2. Energetics of Vacancy Cluster Formation

The relative stabilities of vacancy clusters may be determined using procedures given by Sigler and Kuhlmann-Wilsdorf (1966). For the fcc metals, four types of vacancy cluster morphologies were considered, namely the spherical void, the perfect circular dislocation loop, the faulted (Frank) loop, and the stacking fault tetrahedron. For bcc metals, only the perfect loop, faulted loop, and void were considered. Various equations are available that describe the energy of a dislocation loop. We have chosen the expressions derived by Kroupa (1960), since they are valid for small sizes. The energy of a perfect dislocation loop is given by

$$E_p = \frac{Gb^2}{2(1-\nu)} \{2R + (2R - \varepsilon) [(1 - 0.5\ K^2)\ F(K) - E(K)]\} \qquad (1)$$

where $K^2 = \frac{4R(R-\varepsilon)}{(2R-\varepsilon)^2}$

$$F(K) = \frac{2}{\pi} \int_0^{\pi/2} \frac{d\phi}{\sqrt{1-K^2\sin^2\phi}}$$

$$E(K) = \frac{2}{\pi} \int_0^{\pi/2} d\phi\ \sqrt{1-K^2\sin^2\phi}$$

where G = shear modulus, b = magnitude of the Burgers vector of a perfect loop ($b = a_0/\sqrt{2}$ for fcc and $b = \sqrt{3}\, a_0/2$ for bcc), ν = Poisson's ratio, R = loop radius, and ε = core radius, $\varepsilon \simeq b$. F(K) and E(K) are elliptical integrals of the first and second kind, respectively. They may be solved numerically using polynomial approximations (Abramowitz and Stegun 1972).

A faulted vacancy loop may be described by a similar equation (Kroupa 1960):

$$E_F = \frac{b_F^2}{b^2} E_p + \pi R^2 \gamma \tag{2}$$

where b_F = magnitude of the Burger's vector of a faulted loop ($b_F = a_0/\sqrt{3}$ for fcc and $b_F = a_0/\sqrt{2}$ for bcc), and γ = stacking fault energy. Loop formation is assumed to occur as the result of the collapse of single layers of vacancies on {111} planes in fcc materials and on {110} planes in bcc materials, i.e. the respective close packed planes. The relationship between the number of vacancies (N) and the loop size (R) is given by $R^2 = Na_0^2\, \sqrt{3} / (4\pi)$ for fcc metals and $R^2 = Na_0^2 / (\pi\sqrt{2})$ for bcc metals.

The energy of a stacking fault tetrahedron (SFT) in an fcc metal is given by (Jossang and Hirth 1966)

$$E_T = \frac{Gb^2 L}{6\pi(1-\nu)} \left\{ \ln \frac{4L}{b} + 1.017 + 0.97\, \nu \right\} + \sqrt{3}\, L^2 \gamma \tag{3}$$

where L = tetrahedron edge length. The stacking fault tetrahedron consists of triangular intrinsic stacking faults lying on four intersecting {111} planes. They are believed to form either by direct nucleation of vacancies or by dissociation of a loop onto neighboring {111} planes (Jossang and Hirth 1966).

The formation of SFT in bcc materials does not appear to be possible from geometry considerations. Unlike the close packed {111} planes in fcc metals, the close packed {110} planes in bcc materials do not intersect each other to form a tetrahedron. The relation between the SFT edge length (L) and the number of vacancies is given by $L^2 = Na_o^2 \sqrt{3} / 2$.

The energy of a void may be expressed as (Si-Ahmed and Wolfer 1982)

$$E_v = 4\pi R_v^2 \Gamma \left(1 - \frac{0.8}{N+2}\right) \tag{4}$$

where R_v = void radius, Γ = surface energy of a flat surface, and N = number of vacancies in the void. The term in parenthesis is an empirical correction to the surface energy due to curvature effects and is largely based on computer simulation results of small voids by Mruzik and Russell (1977). The number of vacancies contained in a spherical void is $N = 16\pi R_v^3 / (3a_o^3)$ for fcc metals and $N = 8\pi R_v^3 / (3a_o^3)$ for bcc metals.

3. Results

Values for the materials parameters required in the energy calculations are given in Table 1. These values represent the currently accepted experimental values for the given metals and they include the temperature dependence for the shear modulus, lattice parameter and surface energy. The recommended surface energies for several metals have undergone substantial revision in the past decade as a result of improved testing conditions (Kumikov and Khokonov 1983). The stacking fault energy of both bcc metals was taken to be the calculated value for the {110} fault in iron (Hartley 1966a) and is only considered to be accurate to within a factor of two. Calculations were performed on six fcc metals (gold, silver, aluminum, copper, nickel, and

austenitic stainless steel) and two bcc metals (α-iron and molybdenum) at homologous temperatures near the expected peak void swelling temperature, 0.45 T_M. The effect of temperature on the vacancy cluster energies is rather small, and the calculated results should be reasonably valid over the entire void swelling temperature regime.

Figures 1-6 show the calculated energy per vacancy of the different cluster morphologies as a function of the number of vacancies in the cluster for the six fcc metals. The stacking fault tetrahedron (SFT) is predicted to be the most stable configuration for small ($\lesssim$ 1000 vacancies) clusters in gold, silver, copper and stainless steel, whereas the faulted (smaller sizes) or perfect (larger sizes) vacancy loop is the most stable cluster in aluminum. Void formation in the absence of impurity effects is therefore predicted to never be energetically favorable in these metals. The SFT is the lowest energy geometry in nickel for very small vacancy cluster sizes (< 200 vacancies), while the faulted loop is slightly favored for intermediate sized clusters (300 to 5000 vacancies). The perfect loop is the most stable configuration for all six fcc metals at very large vacancy cluster sizes. Since vacancy cluster nucleation necessarily occurs at small sizes, the stability of the small clusters (< 1000 vacancies) is expected to exert the dominant effect on the final observed morphology. As discussed later, there is an appreciable activation energy barrier that inhibits conversion of vacancy clusters between planar and three-dimensional morphologies. The most interesting aspect of the calculations presented in Figs. 1-6 is that void formation is not expected to occur in any of the high-purity fcc metals investigated.

The calculations for the two bcc metals, α-iron and molybdenum, are presented in Figs. 7 and 8. The faulted loop is predicted to be the most stable

vacancy cluster morphology in α-iron for very small sizes ($\lesssim$ 50 vacancies), with the perfect loop stable at larger sizes. The void is the energetically favored geometry of vacancy clusters in molybdenum up to very large sizes (10,000 vacancies). Calculations by Hartley (1966a,b) and Matthai and Bacon (1984) suggest that the stacking fault energy of Mo may be even greater than that used to construct Fig. 8, which would further enhance the stability of the void in Mo at small cluster sizes. As with the fcc metals, the perfect loop is the preferred vacancy cluster geometry at large sizes for the two bcc metals studied in this investigation.

4. Discussion

Elastic continuum equations are not strictly valid for very small defect clusters (Cotterill 1966), and it would be more appropriate to use atomistic calculations to determine the most stable morphology at cluster sizes where void nucleation is expected to occur ($\lesssim$ 100 vacancies). In particular, the concept of a dislocation loop becomes difficult to envision for sizes < 30 vacancies. Unfortunately, the interatomic potentials of most metals are not known with sufficient accuracy, and atomistic calculations are subject to sizeable errors depending on the choice of interatomic potential and boundary conditions. A direct comparison between atomistic models and the elastic continuum calculations for vacancy clusters is not generally possible at this time due to the lack of quantitative energy per vacancy data for the atomistic case. However, both a recent computer simulation and an anisotropic elasticity calculation of a faulted loop in Fe and Mo containing 37 vacancies give calculated loop energies (37 and 67 eV for Fe and Mo, respectively) that are in good agreement with the elastic continuum energies given in Figs. 7

and 8 (Matthai and Bacon 1984). This indicates that the present elastic continuum results may be accurate at small sizes (N < 200 vacancies) to about ± 10%.

Qualitative atomistic calculations have recently been conducted on the stability of small vacancy clusters in pure copper (Baskes 1977, Doan 1982, Matthai and Bacon 1985). These investigations found that the vacancy loop and SFT (planar configurations) were more stable than the void, in agreement with the continuum calculations (Fig. 4). In addition, computer simulation studies on copper by Savino and Perrin (1974) have shown that planar vacancy clusters collapse and dissociate onto adjoining {111} planes so as to form SFT for sizes as small as 36 vacancies. Vacancy clusters as small as 6 vacancies collapsed to form SFT embryos. These calculations confirm that at least the qualitative trends given in Fig. 4 are valid to very small sizes, i.e. the SFT is energetically favored compared to the faulted loop and void geometries in copper for $N \lesssim 1000$ vacancies. Similar atomistic calculations for nickel by Johnson (1967) found that the void was the most stable morphology for small cluster sizes, in contrast to the prediction of Fig. 5. However, Johnson's results were obtained by assuming an unrealistically high stacking fault energy of 0.30 J/m^2, and they also did not include volume-dependent vacancy formation energy terms which would increase the void energy (Savino and Perrin 1974). This points out that caution must be exercised when using the results from atomistic calculations. The most important aspect of the continuum calculations presented in this paper are their qualitative predictions of the energetically favored cluster geometry at small sizes for the different metals.

4.1 Activation Energy for the Collapse of a Void

At very large sizes, the perfect loop is always the most energetically stable type of vacancy cluster. Therefore, voids which may have been energetically stable at small sizes may become unstable once they have grown larger than a critical size. It is important to determine the probability that a void of a given size will collapse into a planar defect cluster. An activation energy barrier exists that inhibits conversion of a void to a dislocation loop due to the increase in surface area (and, thereby, total surface energy) associated with the conversion process. An upper limit to this activation energy barrier is obtained by comparing the energy difference between a sphere and a disk (of thickness b) that are of equal volume:

$$\Delta E = E_v \left[\frac{2R_v}{3b} - 1\right] \tag{5}$$

A somewhat more realistic estimate of the activation energy may be obtained by comparing the total surface energies of a sphere and an oblate spheroid (Beyer 1978). The oblate spheroid more accurately represents the geometry of a void that is in the process of collapsing to a planar configuration. The energy difference is given by

$$\Delta E = C \cdot E_v \tag{6}$$

where C is a geometric constant that depends on the eccentricity of the spheroid and E_v is given by Eq. (4). Values of C are given in Table 2 for various ratios of major to minor axis along with calculated activation energies per vacancy for the collapse of a "typical" small void.

The collapse of a void requires the collective motion of atoms lying on its surface. In particular, the geometric change from a sphere of radius R to an oblate spheroid of minor radius c requires the rearrangement of N_s surface atoms, where $N_s \simeq 16\pi R^2 (R-C)/(3\ a_o^3)$. Therefore, the overall surface energy barrier for the collapse of a void (effective activation energy) is approximately equal to $N_s \quad \Delta E$, where ΔE is given by Eq. (6). The effective energy barrier for the collapse of a void containing 100 vacancies is also given in Table 2. A rule-of-thumb in void nucleation calculations is that energy barriers up to 50 kT may occasionally be surmounted by thermal energy processes. For temperatures applicable to void swelling in metals, this indicates that energy barriers $\gtrsim$ 4 eV will not allow void collapse to occur. Since the activation energy barrier is proportional to R_v^2, it is suggested from Table 2 that void collapse will not occur except possibly for voids that have just nucleated and are, therefore, very small (R_v < 1 nm).

The preceding calculations of the activation energy for void collapse do not consider the effect of attractive forces between the facing planes of the partially collapsed vacancy cluster, which should decrease the energy barrier for void collapse. If one assumes that an interplanar separation of $\lesssim$ 0.4 nm ($c \lesssim 0.2$ nm) will produce complete collapse of a vacancy cluster, then calculations similar to those in Table 2 predict that voids containing less than 60 vacancies should collapse for the case of copper. Voids containing more than 100 vacancies are predicted to be stable against collapse. Of course, these calculations are only crude estimates that need to be confirmed by atomistic models. Molecular dynamics studies of copper have determined that a spherical void containing 42 vacancies collapses to a loop or SFT at 800 and

500 K, but not at 0 K, which is in agreement with the present calculations (Protasov and Chudinov 1982, Matthai and Bacon 1985).

4.2 Comparison of Calculations with Experimental Observations

The motivation for this study is that, while void formation has been commonly observed in a wide variety of metals in the past, there have been occasional reports where greatly reduced or no void formation has been observed. It has often been assumed that the difference in these observations is due to impurity or solute atom effects. Impurity and solute effects have been invoked to explain both enhanced and reduced swelling observations in metals. An important question is whether voids are energetically stable in "pure" metals (Harkness and Li 1969, Bullough and Perrin 1969). Previous calculational studies attempted to address this question with limited success (Cotterill 1966, Sigler and Kuhlmann-Wilsdorf 1966, Buswell 1970). These earlier studies were hampered by incorrect data for the metal surface energies, etc. and also by the lack of careful experimental studies on quenched or irradiated high purity metals. We have taken care in this paper to use the best measurements of material properties data that are currently available. In general, the agreement is good between the present calculations and recent experimental observations in well-characterized metals with regard to the most stable vacancy cluster morphology. It appears that discrepancies can generally be attributed to impurity effects. The calculated and observed stable vacancy cluster geometry are compared for each individual metal below.

Experimentally, both SFT and Frank loops have been observed in quenched and mechanically deformed gold (Silcox and Hirsch 1959, Loretto, Clarebrough and Segall 1965, Eyre 1973). Irradiation studies have also generally found that the SFT is the most stable vacancy cluster form in Au (Suehiro, Yoshida

and Kiritani 1982, Shimomura et al. 1985). These findings are in agreement with Fig. 1 where SFT and, over a limited range, Frank loops are calculated to be the most stable geometry. However, Yoshida et al. (1965) and Clarebrough et al. (1967) observed some void formation in addition to the customary SFT in quenched gold. It was suggested that the existence of voids in quenched gold may be due to impurity gas effects (Clarebrough et al. 1967).

In agreement with Fig. 2, SFT and vacancy loops have been commonly observed in quenched, deformed or irradiated silver (Smallman, Westmacott and Coiley 1959, Loretto et al. 1965, Eyre 1973, Kitagawa et al. 1985). Void formation has also been observed in quenched silver under certain circumstances (Clarebrough et al. 1967, Eyre 1973). The void density was strongly influenced by the quenching atmosphere. Both oxygen and hydrogen were observed to promote void formation (Clarebrough et al. 1967). A low density of voids was also observed following a vacuum quench, but the vacuum pressure was rather high (10^{-6} torr) and the identity of the residual gases was not given.

Faulted and perfect loops are commonly observed in quenched or irradiated high-purity aluminum (Smallman et al. 1959, Strudel, Vincotte and Washburn 1963, Eyre 1973, McLaurin 1984). In contrast to Au and Ag, there have been no known observations of SFT in aluminum. These observations are in agreement with the calculations presented in Fig. 3. McLaurin (1984) observed that electron irradiation of high-purity aluminum resulted in the formation of faulted vacancy loops (with no associated void formation). Subsequent growth during continuous irradiation caused the faulted loops to shear and become perfect loops, as predicted by Fig. 3. Similar observations were reported by Strudel et al. (1963) for quenched aluminum. The transition between faulted and perfect loops in aluminum occurs at a loop diameter of $\lesssim$ 15 nm (2500

vacancies), which indicates that there is an energy barrier to the unfaulting process according to Fig. 3. The loop shear activation energy in aluminum has been estimated to be greater than 1 to 1.7 eV (Saada 1963, Kuhlmann-Wilsdorf 1965). Void formation has been observed by several investigators in quenched or irradiated aluminum (Das and Washburn 1965, Westmacott, Smallman and Dobson 1968, Eyre 1973). Shimomura and Yoshida (1967) have shown that void formation in quenched aluminum is due to gas effects, in particular hydrogen.

As predicted in Fig. 4, there have been a number of reported observations of SFT in quenched, deformed or irradiated high-purity copper (Loretto et al. 1965, Clarebrough, Segall and Loretto 1966, English 1982, Suehiro et al. 1982, Yoshida, Akashi and Kitajima 1985, Zinkle, Kulcinski and Knoll 1985). Other investigations have found voids instead of SFT in quenched or irradiated copper (Clarebrough et al. 1967, Bowden and Ballufi 1969, Glowinski 1976). Glowinski found that void formation did not occur in copper foils that had been vacuum annealed (degassed) prior to their irradiation, in contrast to "non-degassed" foils. Similar gas effect observations have been found in quenched copper (Clarebrough et al. 1967). A model is developed in the accompanying paper (Part II) which predicts that oxygen concentrations as low as 1 wt. ppm may stabilize void formation in copper (oxygen is a common impurity in copper).

Vacancy loops and SFT have been observed in quenched or irradiated high purity nickel (Smallman et al. 1959, Humble, Loretto and Clarebrough 1967, Brimhall 1974, Kiritani, Yoshida and Ishino 1984, Yoshida et al. 1985). This matches the predictions of Fig. 5. Void formation has also been observed in irradiated Ni in many cases (Kulcinski, Brimhall and Kissinger 1972, Bullen 1984). However, void formation in nickel is also known to be related to gas

effects (Bullen 1984). The calculations presented in this paper have utilized recent stacking fault energy (s.f.e.) measurements (Pavlov et al. 1984, Carter and Holmes 1977, Narita et al. 1977) which are substantially lower than previous values for nickel (Gallagher 1970). Calculations using the older s.f.e. value result in the same general conclusions regarding vacancy cluster stability in nickel, i.e. the SFT and faulted loop are the preferred vacancy cluster geometries at small and intermediate sizes.

Figure 6 predicts that the SFT is the most stable vacancy cluster morphology in austenitic stainless steel. This is in contrast to numerous studies which found that void formation occurred in stainless steel following quenching or charged particle irradiation (Ballufi and Seidman 1972, Packan and Farrell 1982). However, other researchers have observed SFT either alone or in conjunction with voids in quenched, deformed and irradiated austenitic stainless steels (Artigue, Condat and Fayard 1977, Kiritani et al. 1984, Sindelar 1985, Yoshida et al. 1985). The oxygen content in the steel apparently plays an important role in determining the preferred vacancy cluster geometry. Sindelar (1985) found that void formation was greatly reduced in a "low-oxygen" 316 stainless steel alloy compared to a "high-oxygen" alloy. Formation of SFT was observed in the low-oxygen alloy, and void formation was completely suppressed in a specimen that had been "degassed" by a vacuum anneal prior to irradiation. These observations once again highlight the important consequences of small levels of reactive gases which are commonly introduced into metals during the fabrication process.

Figure 7 indicates that the faulted loop with b = a/2 <110> is the favored vacancy cluster geometry in pure iron for sizes up to 50 vacancies (R_L = 1 nm). The maximum size for a stable faulted loop may be less than

50 vacancies due to uncertainties in the stacking fault energy for α-Fe, as discussed earlier. Computer calculations to date with regard to faulted loop stability in bcc metals indicate that {110} faults are unstable, whereas {112} double layer faults are stable (Matthai and Bacon 1984, Esterling et al. 1984). However, recent experimental observations of vacancy loops in bcc metals indicate that nucleation may likely occur on a {110} plane, with subsequent shearing to a perfect loop (Eyre and English, 1982). There are no known observations to date of faulted loops in iron, but there have been several observations of perfect vacancy loops that are consistent with the concept of faulted (b = a/2 <110>) loops unfaulting at small sizes to form perfect loops with b = a/2 <111> or b = a <100> (Kayano et al. 1978, Robertson, Jenkins and English 1982, Eyre and English 1982). Other irradiation studies have observed void formation in iron instead of vacancy loops (Smidt et al. 1973, Kitajima, Futagami and Kuramoto 1979, DeSchepper, Knuyt and Stals 1984). The existence of voids in irradiated iron may very well be due to impurity effects. Hondros (1968) has observed that oxygen (which is commonly contained in even high-purity iron) has a very strong effect on the surface energy of iron under conditions where surface chemisorption occurs. Therefore, oxygen impurities could lower the Fe surface energy at low and intermediate temperatures where oxygen solubility in the matrix is small and, thereby, stabilize void formation in a manner similar to that described in the accompanying paper (Part II).

Similar to the case for iron, the vacancy cluster geometry in molybdenum has been observed to be either the void or the perfect loop. Perfect vacancy loops with b = a <100> or b = a/2 <111> have been observed in quenched or irradiated Mo by several researchers (Meakin, Lawley and Koo 1965, Eyre and

English 1982, Stubbins 1984). In addition, Evans, Van Veen and Caspars (1983) observed helium filled vacancy cluster plates on {110} planes in He-irradiated molybdenum. This morphology is in contrast to the stability predictions given in Fig. 8. There have been numerous observations of voids in irradiated high-purity molybdenum (Rau, Ladd and Moffett 1969, Kulcinski et al. 1972, Eldrup, Mogensen and Evans 1976, Brimhall, Simonen and Charlot 1984), in agreement with Fig. 8. Stubbins (1984) observed that electron irradiation of Mo created vacancy loops for temperatures $\leq$ 850°C and voids at 900°C. This is an indication that kinetic effects (which are not treated in this paper) may have some control over the prevalent vacancy cluster geometry at low temperatures. An alternative explanation is that the material properties data for Mo may be in error, and that the void and loop geometries are of approximately equal energy. It is uncertain what effect impurities may have on the Mo surface energy, but it is likely that impurities will decrease its value in a manner similar to that seen for other metals. The best surface energy measurements of Mo to date (Kumikov and Khokonov 1983) have been made under conditions where a sizeable impurity concentration may still exist. Loop formation would be predicted to occur if the surface energy for high-purity Mo was increased to about 3.8 J/m^2.

The general agreement between theory (Figs. 1-8) and experiments performed on pure metals (with the possible exception of molybdenum) indicates that the continuum calculation method is at least qualitatively correct in its stability predictions at small cluster sizes. However, experimental observations conclusively show that the actual vacancy cluster geometry can vary among several possibilities depending on the presence of small levels of impurities (Clarebrough et al. 1967, Shimomura and Yoshida 1967, Glowinski

1976). In order to examine this variability of experimental results, it is necessary to include the effect of impurities on the relative energies of vacancy clusters. Future vacancy cluster studies in metals should pay close attention to the impurities that may be present, including the often-neglected interstitial impurities H, C, N and O. Wehner and Wolfer (1985) concluded that gas is not needed for vacancy cluster nucleation, but gaseous impurities may prevent the collapse of vacancy clusters into loops (thereby stabilizing void formation). A model is developed in the companion paper that addresses the effect of oxygen and helium on the vacancy cluster energies.

Acknowledgements

The authors would like to thank P. Caliva for her assistance in preparing this paper. This work was supported by the U.S. Department of Energy.

References

Abramowitz, M. and Stegun, I.A., 1972, Handbook of Mathematical Functions, (Dover) p. 591.

Artigue, F., Condat, M. and Fayard, M., 1977, Scr. Metall., 11, 623.

Ballufi, R.W. and Seidman, D.N., 1972, in Radiation Induced Voids in Metals, Eds. Corbett, J.W. and Ianniello, L.C., USAEC CONF-710601, p. 563.

Baskes, M.I., 1977, Trans. Amer. Nucl. Soc., 27, 320.

Beyer, W.H., Ed., 1978, CRC Standard Mathematical Tables, 25th Ed. (CRC Press) p. 149.

Bowden, H.G. and Ballufi, R.W., 1969, Phil. Mag., 19, 1001.

Brimhall, J.L., 1974, Battelle Northwest Lab. Report BNWL-1839.

Brimhall, J.L., Simonen, E.P. and Charlot, L.A., 1984, J. Nucl. Mat., 122 & 123, 579.

Bullen, D.B., 1984, Ph.D. Thesis, "The Effects of Implanted Hydrogen and Helium on Cavity Formation in Self-Ion Irradiated Nickel", Nuclear Engineering Dept., University of Wisconsin-Madison.

Bullen, D.B., Kulcinski, G.L. and Dodd, R.A., 1985, J. Nucl. Mat., 133 & 134, 455.

Bullough, R. and Perrin, R.C., 1969, in Rad. Damage in Reactor Mater., Vol. II (IAEA, Vienna) p. 233.

Buswell, J.T., 1970, CEGB Report RD/B/N-1584, Berkeley Nucl. Lab.

Carter, C.B. and Holmes, S.M., 1977, Phil. Mag., 35, 1161.

Clarebrough, L.M., Humble, P. and Loretto, M.H., 1967, Acta Met., 15, 1007.

Clarebrough, L.M., Segall, R.L. and Loretto, M.H., 1966, Phil. Mag., 13, 1285.

Cotterill, R.M.J., 1966, in The Nature of Small Defect Clusters, Vol. 1 (Consultants Symp.), Ed. Makin, M.J., Harwell Report AERE R5269, p. 144.

Das, G. and Washburn, J.W., 1965, Phil. Mag., 11, 955.

DeSchepper, I., Knuyt, G. and Stals, L.M., 1984, J. Nucl. Mat., 122 & 123, 590.

Doan, N.V., 1982, in Point Defects and Defect Interactions in Metals, Eds. Takamura, J-I., Doyama, M. and Kiritani, M., (Univ. of Tokyo Press) p. 722.

Eldrup, M., Mogensen, O.E. and Evans, J.H., 1976, J. Phys. F., 6(4), 499.

English, C.A., 1982, J. Nucl. Mat., 108/109, 104.

Esterling, D.M., McGurn, A.R., Boswarva, I.M. and Arsenault, R.J., 1984, Mat. Sci. Eng., 68, 97.

Evans, J.H., Van Veen, A. and Caspars, L.M., 1983, Rad. Effects, 78, 105.

Eyre, B.L., 1973, J. Phys. F: Metal Phys., 3, 422.

Eyre, B.L. and English, C.A., 1982, in Point Defects and Defect Interactions in Metals, Eds. Takamura, J-I., et al. (Univ. Tokyo Press) p. 799.

Gallagher, P.C.J., 1970, Met. Trans. 1, 2429.

Glowinski, L.D., 1976, J. Nucl. Mat. 61, 8.

Guinan, M.W. and Steinberg, D.J., 1974, J. Phys. Chem. Sol., 35, 1501.

Harkness, S.D. and Li, Che-Yu, 1969, in Radiation Damage in Reactor Materials, Vol. II, Vienna, IAEA, p. 189.

Hartley, C.S., 1966a, Phil. Mag., 14, 7; 1966b, Acta Met., 14, 1133.

Hondros, E.D., 1968, Acta. Metall., 16, 1377.

Humble, P., Loretto, M.H. and Clarebrough, L.M., 1967, Phil. Mag., 15, 297.

Johnson, R.A., 1967, Phil. Mag., 16, 553.

Jossang, T. and Hirth, J.P., 1966, Phil. Mag., 13 , 657.

Kayano, H., Yoshinaga, H., Abe, K. and Morozumi, S., 1978, J. Nucl. Sci. Technol., 15, 200.

Kiritani, M., Yoshida, N. and Ishino, S., 1984, J. Nucl. Mat., 122 & 123, 602.

Kitagawa, K., Yamakawa, K., Fukushima, H., Yoshiie, T., Hayashi, Y., Yoshida, H., Shimomura, Y. and Kiritani, M., 1985, J. Nucl. Mater., 133 & 134, 395.

Kitajima, K., Futagami, F. and Kuramoto, E., 1979, J. Nucl. Mat., 85 & 86, 725.

Kittel, C., 1976, Introduction to Solid State Physics, 5th Ed., (John Wiley and Sons) p. 31.

Kroupa, F., 1960, Czech J. Phys., 10B, 284.

Kuhlmann-Wilsdorf, 1965, in Lattice Defects in Quenched Metals, Eds. Cotterill, R.M.J., Doyama, M., Jackson, J.J. and Meshii, M. (Academic Press) p. 269.

Kulcinski, G.L., Brimhall, J.L. and Kissinger, H.E., 1972, in Radiation-Induced Voids in Metals, Eds. Corbett, J.W. and Ianniello, L.C. (USAEC CONF-710601) p. 449.

Kumikov, V.K. and Khokonov, Kh.B., 1983, J. Appl. Phys., 54, 1346.

Loretto, M.H., Clarebrough, L.M. and Segall, R.L., 1965, Phil. Mag., 11, 459.

Matthai, C.C. and Bacon, D.J., 1984, J. Nucl. Mat. 125, 138.

Matthai, C.C. and Bacon, D.J., 1985, J. Nucl. Mat. 135, 173.

McLaurin, S.K., 1984, Ph.D. Thesis, "Radiation Damage from Heavy Ion Bombardment in High Purity Aluminum", Nuclear Engineering Department, University of Wisconsin-Madison.

Meakin, J.D., Lawley, A. and Koo, R.C., 1965, in Lattice Defects in Quenched Metals, Eds. Cotterill, R.M.J., Doyama, M., Jackson, J.J. and Meshii, M., (Academic Press) p. 767.

Mruzik, M.R. and Russell, K.C., 1977, Surf. Sci., 67, 205.

Narita, N., Hatano, A., Takamura, J., Yoshida, M. and Sakamoto, H., 1978, J. Jap. Inst. Met., 42, 533.

Packan, N.H. and Farrell, K., 1982, in Effects of Radiation on Materials, 11th Conf., Eds. Brager, H.R. and Perrin, J.S., ASTM STP 782, p. 885.

Pavlov, V.A., Shalaev, V.I. and Alyabiev, V.M., 1984, Phys. Stat. Sol. a, 85, 11.

Protasov, V.I. and Chudinov, V.G., 1982, Rad. Effects, 66, 1.

Rau, R.C., Ladd, R.L. and Moffett, J., 1969, J. Nucl. Mat., 33, 324.

Reed, R.P. and Schramm, R.E., 1974, J. Appl. Phys., 45, 4705.

Rhodes, C.G. and Thompson, A.W., 1977, Met. Trans., 8A, 1901.

Robertson, I.M., Jenkins, M.L. and English, C.A., J. Nucl. Mat., 108 & 109, 209.

Saada, G.V., 1963, Proc. Intern. Conf. Crystal Lattice Defects, J. Phys. Soc. Japan, Suppl. III, 18, 41.

Savino, E.J. and Perrin, R.C., 1974, J. Phys. F, 4, 1889.

Shimomura, Y. and Yoshida, S., 1967, J. Phys. Soc., Japan, 22, 319.

Shimomura, Y., Yoshida, H., Kiritani, M., Kitagawa, K. and Yamakawa, K., 1985, J. Nucl. Mat., 133 & 134, 385.

Si-Ahmed, A. and Wolfer, W.G., 1982, in Effects of Radiation on Materials: 11th Conf., Eds. Brager, H.R. and Perrin, J.S., ASTM STP 782, p. 1008.

Sigler, J.A. and Kuhlmann-Wilsdorf, D., 1966, in The Nature of Small Defect Clusters, Vol. 1, Ed. Makin, M.J., Harwell Report AERE R5269, p. 125.

Silcox, J. and Hirsch, P.B., 1959, Phil Mag., 4, 72.

Sindelar, R.L., 1985, "A Comparison of the Response of 316 SS and the P7 Alloy to Heavy-Ion Irradiation", Ph.D. Thesis, Nuclear Engineering Department, University of Wisconsin-Madison.

Smallman, R.E., Westmacott, K.H. and Coiley, J.H., 1959, J. Inst. Metals, 88, 127.

Smidt, F.A., Jr., Sprague, J.A., Westmoreland, J.E. and Malmberg, P.R., 1973, in Defects in B.C.C. Metals and Their Alloys, Nuclear Metallurgy, Vol. 18, Ed. Arsenault, R.J., National Bureau of Standards p. 341.

Smithell's Metal Reference Book, 1983, Ed. Brandes, E.A. (Butterworth) p. 15-2.

Strudel, J.L., Vincotte, F. and Washburn, J. 1963, Appl. Phys. Letters, 3, 148.

Stubbins, J.F., 1984, J. Nucl. Mat., 122 & 123, 715.

Suehiro, M., Yoshida, N. and Kiritani, M., 1982, in Point Defects and Defect Interactions in Metals, Eds. Takamura, J-I., et al. (Univ. Tokyo Press) p. 795.

Tyson, W.R., 1975, Can. Metall. Quart, 14, 307.

Weast, R.C., 1979, CRC Handbook of Chemistry and Physics.

Wehner, M.F. and Wolfer, W.G., 1985, Phil. Mag. A, 52, 189.

Westmacott, K.H., Smallman, R.E. and Dobson, P.S., 1968, Met. Sci. J., 2, 177.

Yoshida, N., Akashi, Y. and Kitajima, K., 1985, J. Nucl. Mat., 133 & 134, 405.

Yoshida, S., Kiritani, M., Shimomura, Y. and Yoshinaka, A., 1965, J. Phys. Soc. Japan, 20, 628.

Zinkle, S.J., Kulcinski, G.L. and Knoll, R.W., 1985, J. Nucl. Mat. (in press).

Zinkle, S.J., Wolfer, W.G., Kulcinski, G.L. and Seitzman, L.E., 1985, submitted to Phil. Mag.

Table 1. Materials Parameters at 0.45 T_M

Metal	G (GPa)	ν	a_o (nm)	γ (J/m^2)	Γ (J/m^2)
Au	25.4	0.42	.410	0.050	1.51 @ 335°C
Ag	26.5	0.37	.411	0.022	1.29 @ 280°C
Al	24.2	> 0.33	.406	0.163	1.14 @ 150°C
Cu	42.1	0.355	.363	0.062	1.64 @ 340°C
Ni	72.4	0.312	.354	0.150	2.12 @ 510°C
Stainless Steel	57.6	0.30	.363	0.040	2.20 @ 530°C
α-Fe	60.3	0.293	.289	0.75	2.32 @ 540°C
Mo	106	0.293	.317	0.75	2.81 @ 1030°C

Notes: (1) Values for G(T) and ν from Guinan and Steinberg (1974) and Smithell (1983). (2) Values for a_o(T) from Kittel 1976 and Weast 1979. (3) Values for γ from Gallagher 1970, Reed and Schramm 1974, Rhodes and Thompson 1977 (fcc) and Hartley 1966a (bcc). (4) Values for Γ(T) from Kumikov and Khokonov (1983) and Tyson 1975. (5) Γ for stainless steel is value of γ-Fe. (6) γ for Mo is value for α-Fe.

Table 2. Surface Energy Barrier for the Collapse of a Void in Copper

	Oblate Spheroid			Disk
	a/c = 2	a/c = 4	a/c = 6	
Energy Barrier Constant, C*	0.095	0.43	0.88	$\frac{2R_v}{3b} - 1$
Activation Energy per Vacancy, ΔE**	0.03 eV	0.14 eV	0.29 eV	0.37 eV
Effective Energy Barrier	1 eV	8 eV	20 eV	24 eV

a/c = ratio of major/minor axis

*In terms of the initial void energy

** Assuming R_v = 0.7 nm (100 vacancies) and Γ = 1 J/m^2

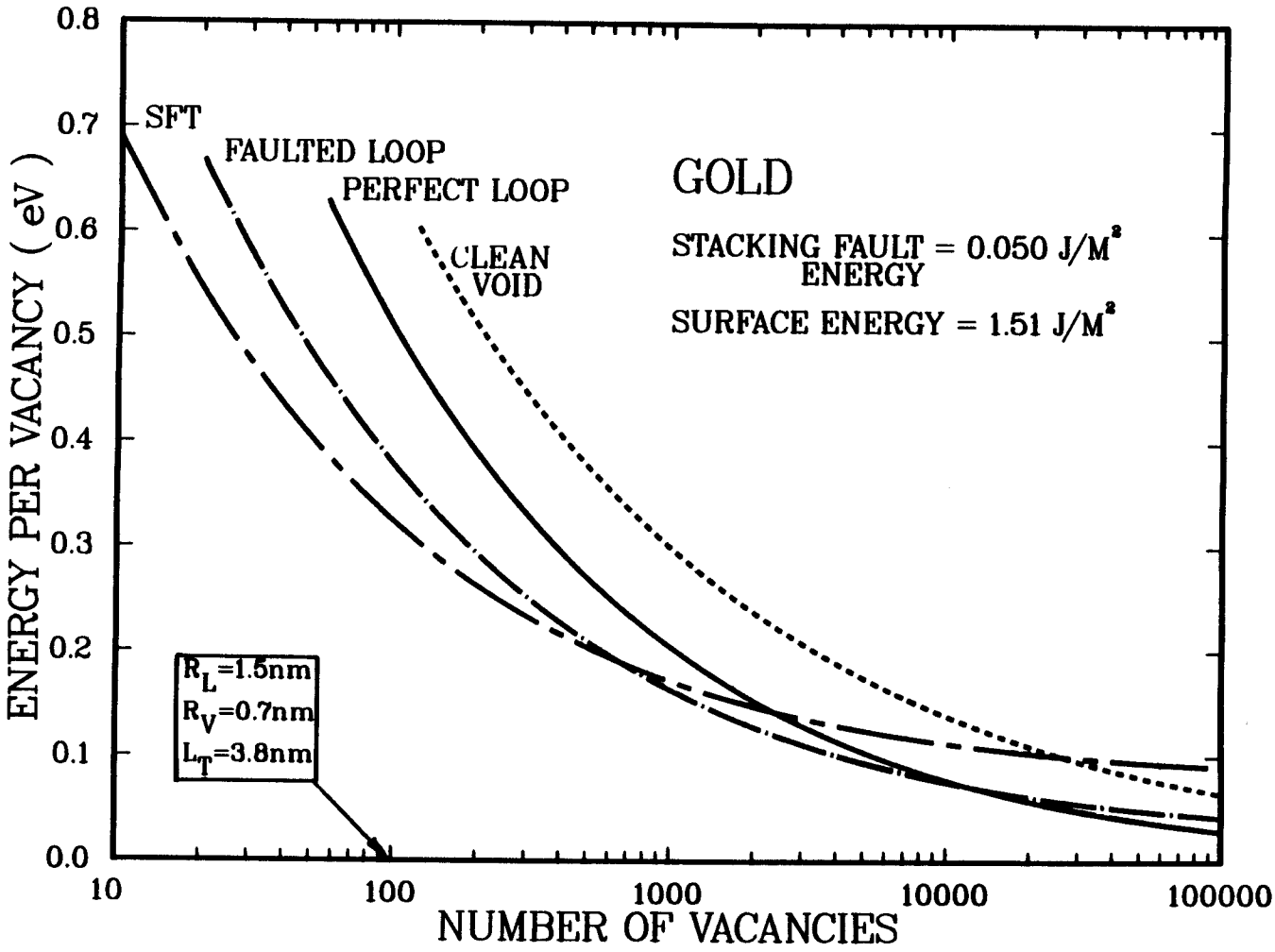

Figure 1. Calculated specific energies of vacancy clusters in pure gold.

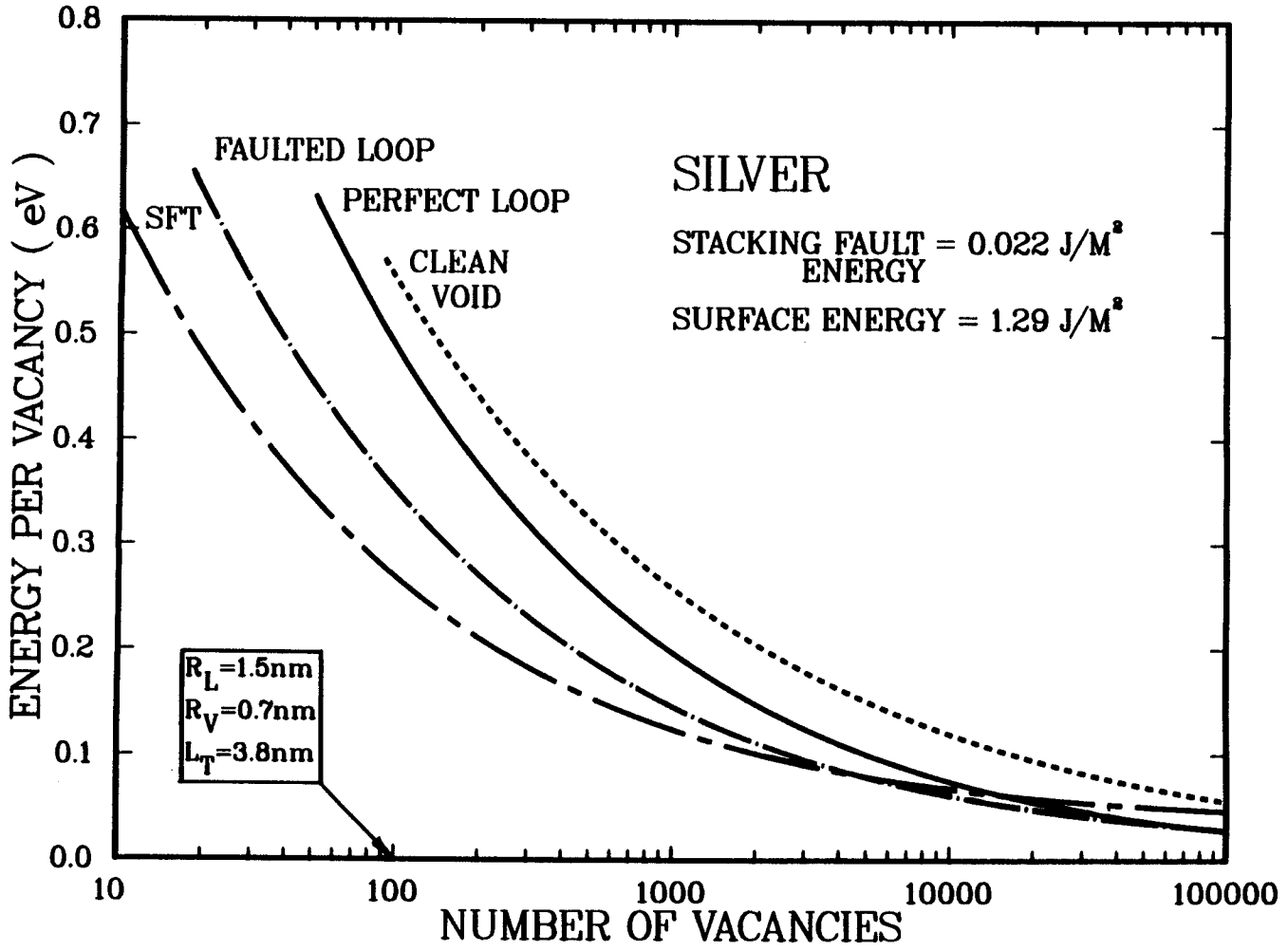

Figure 2. Calculated specific energies of vacancy clusters in pure silver.

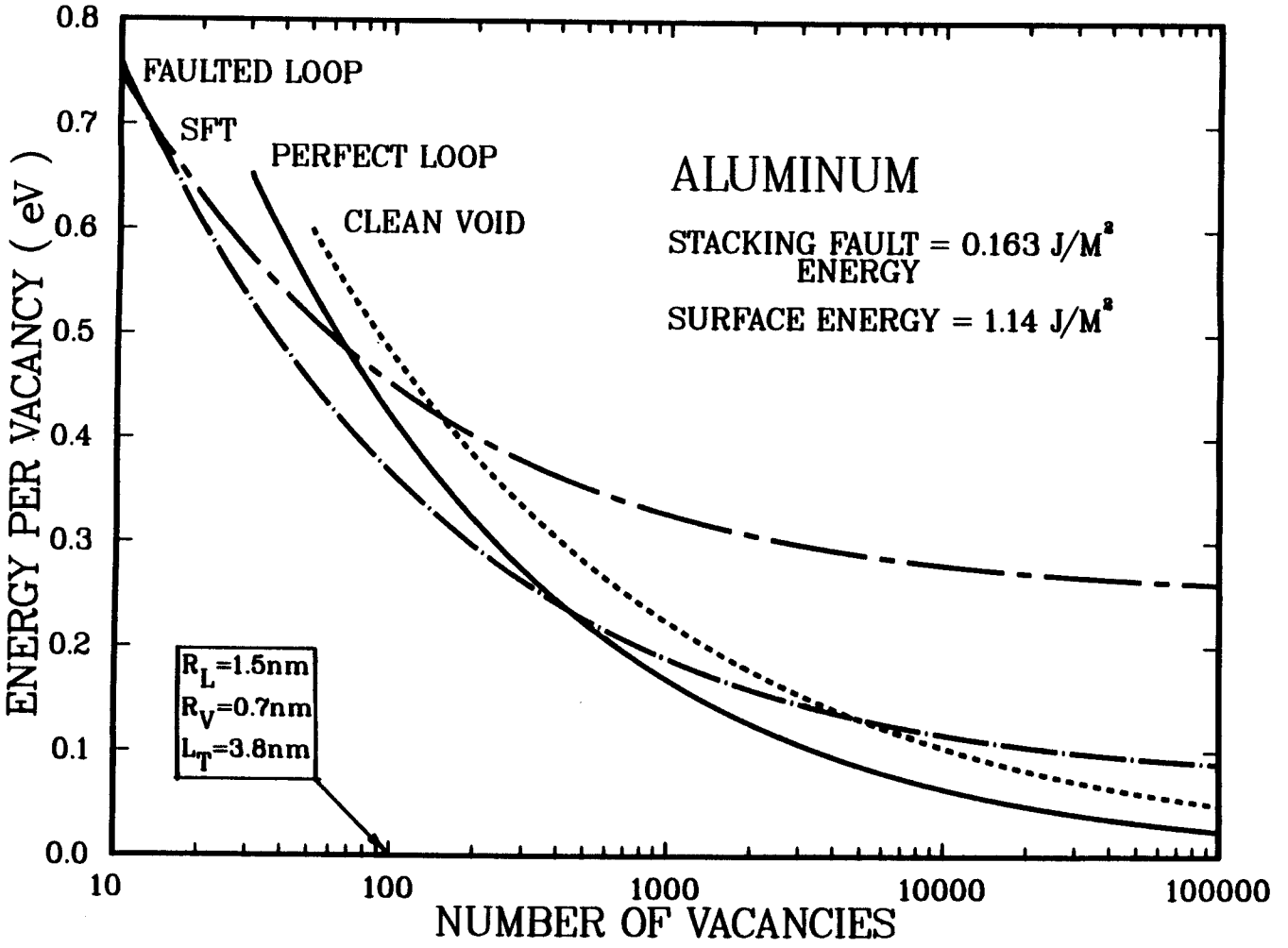

Figure 3. Calculated specific energies of vacancy clusters in pure aluminum.

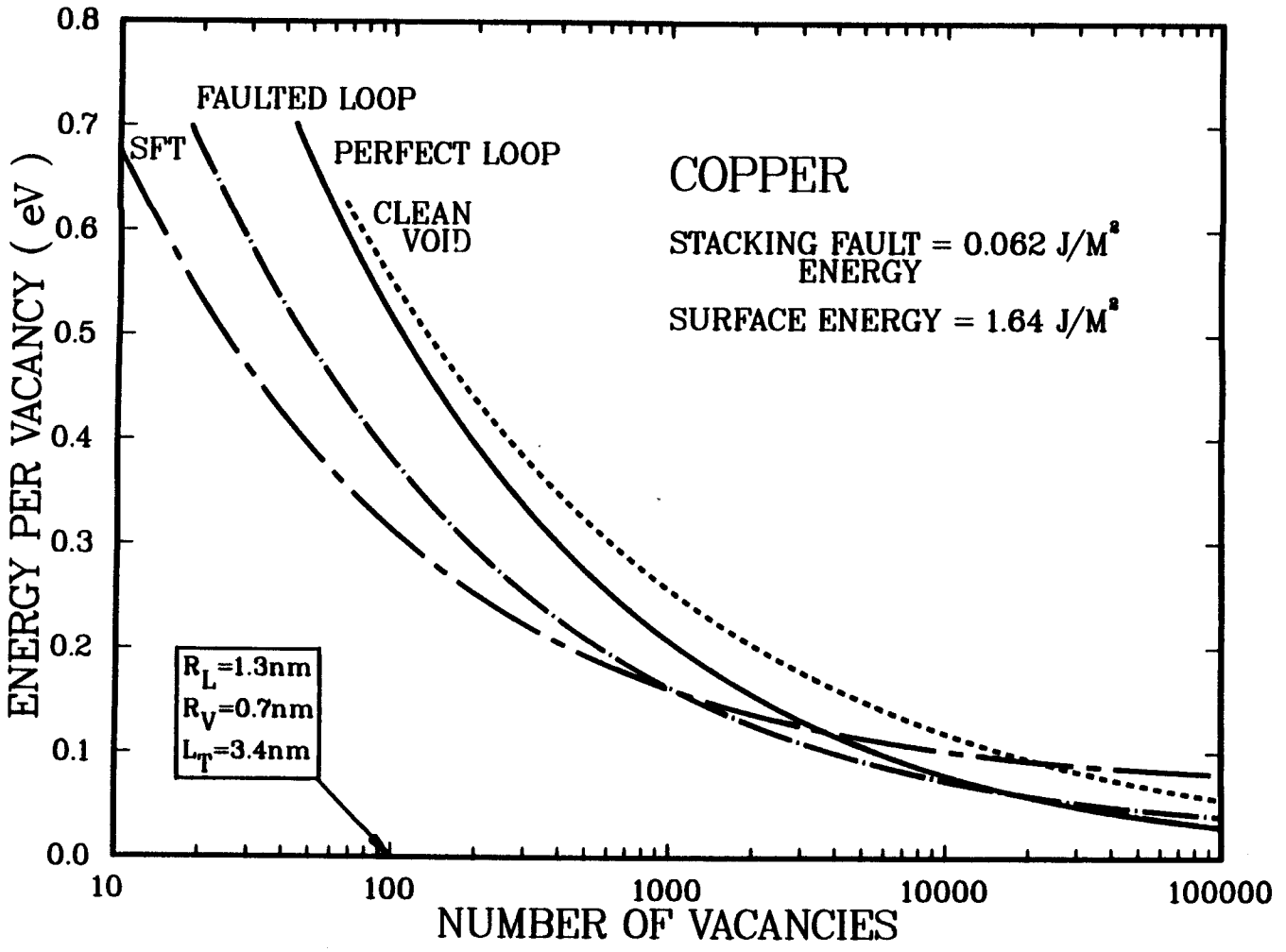

Figure 4. Calculated specific energies of vacancy clusters in pure copper.

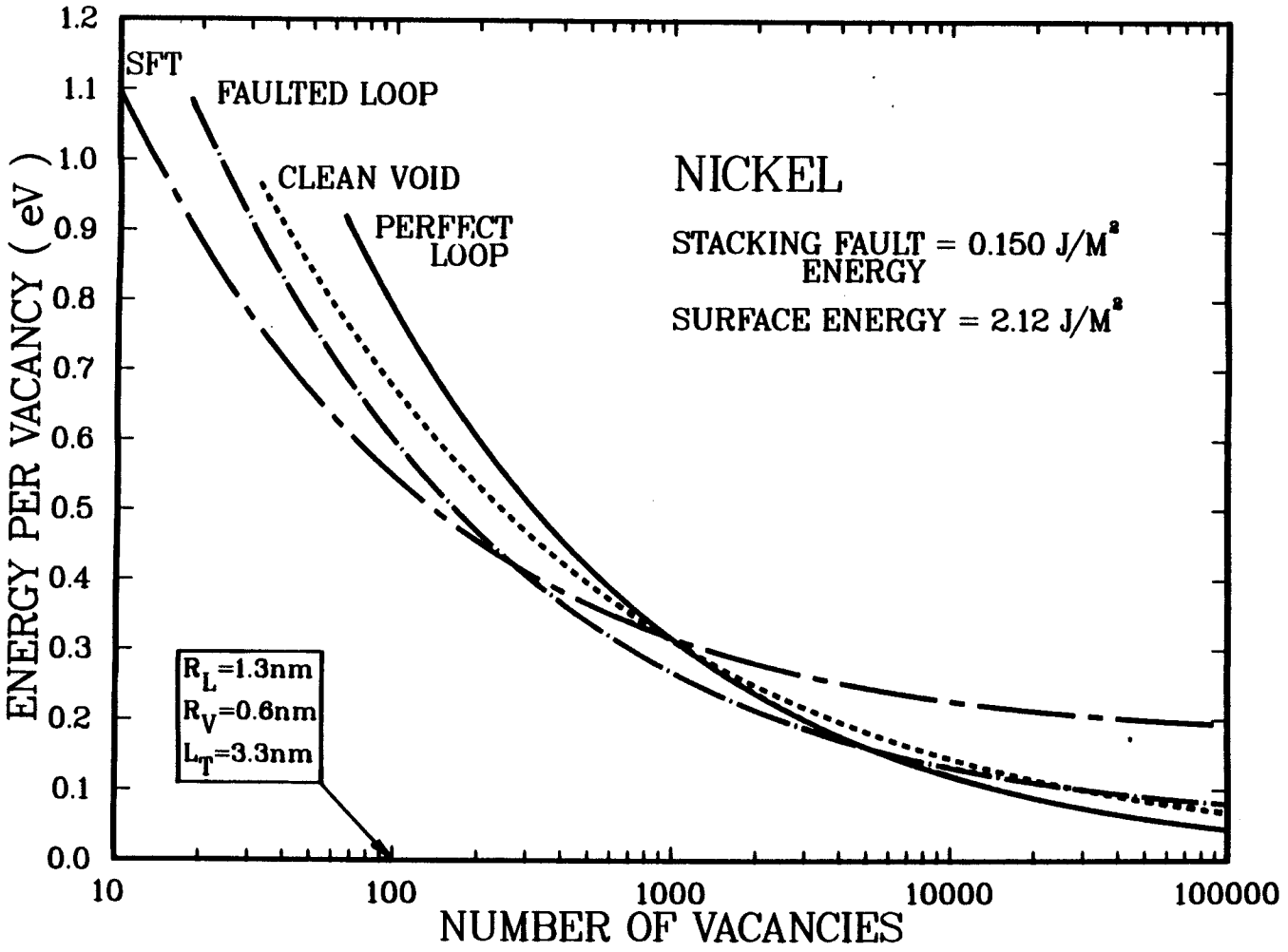

Figure 5. Calculated specific energies of vacancy clusters in pure nickel.

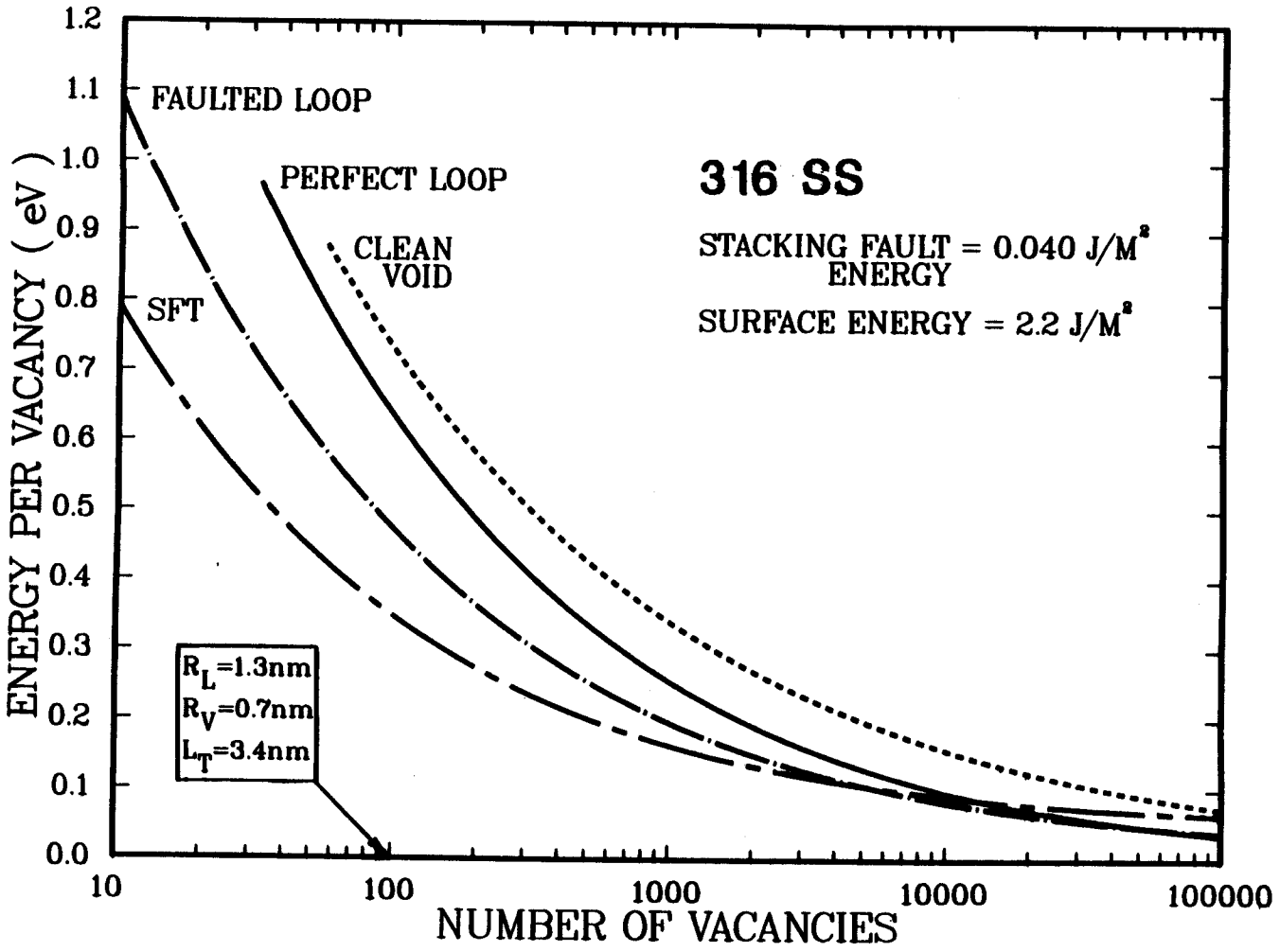

Figure 6. Calculated specific energies of vacancy clusters in 316 stainless steel.

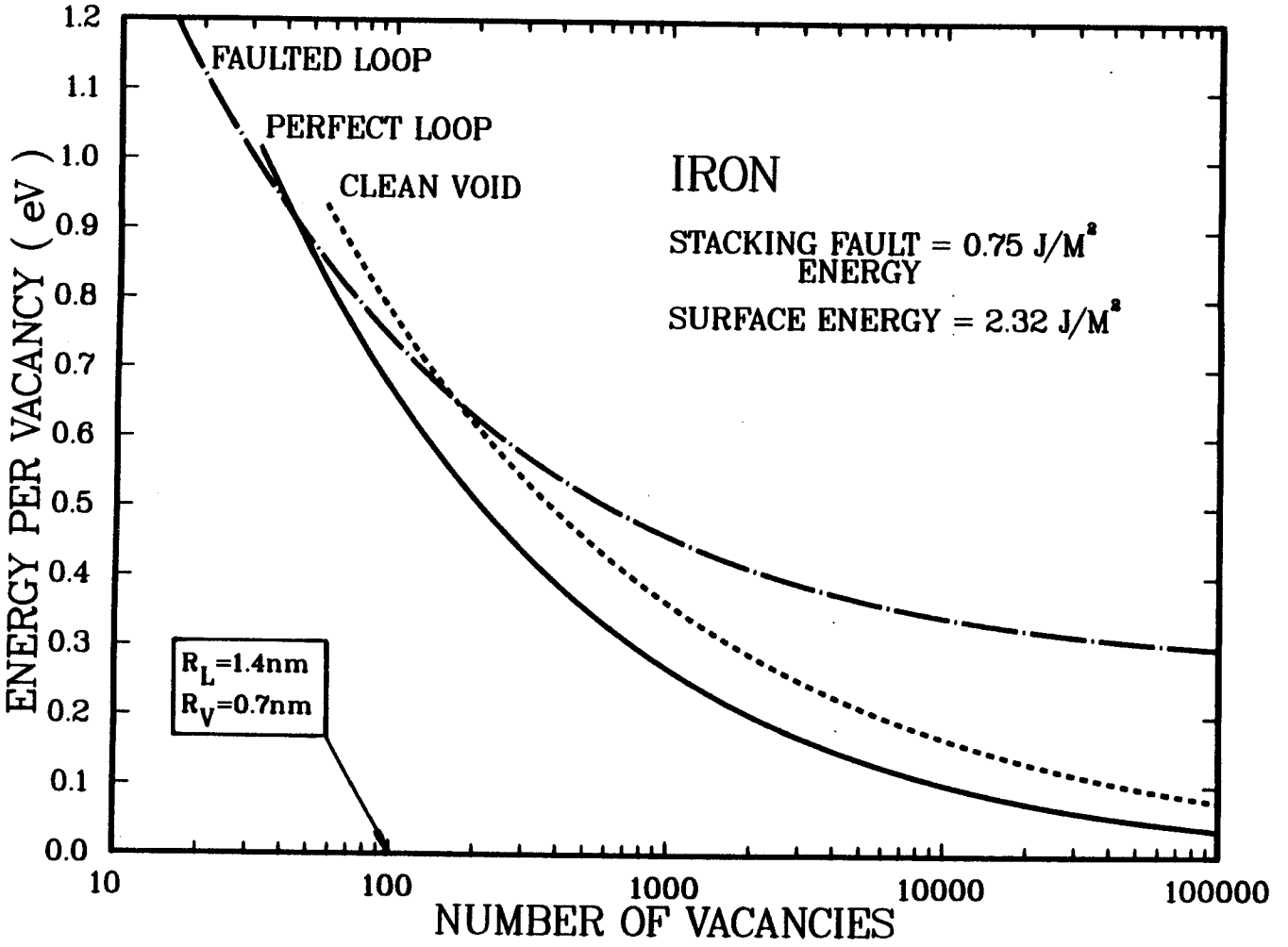

Figure 7. Calculated specific energies of vacancy clusters in pure iron (bcc).

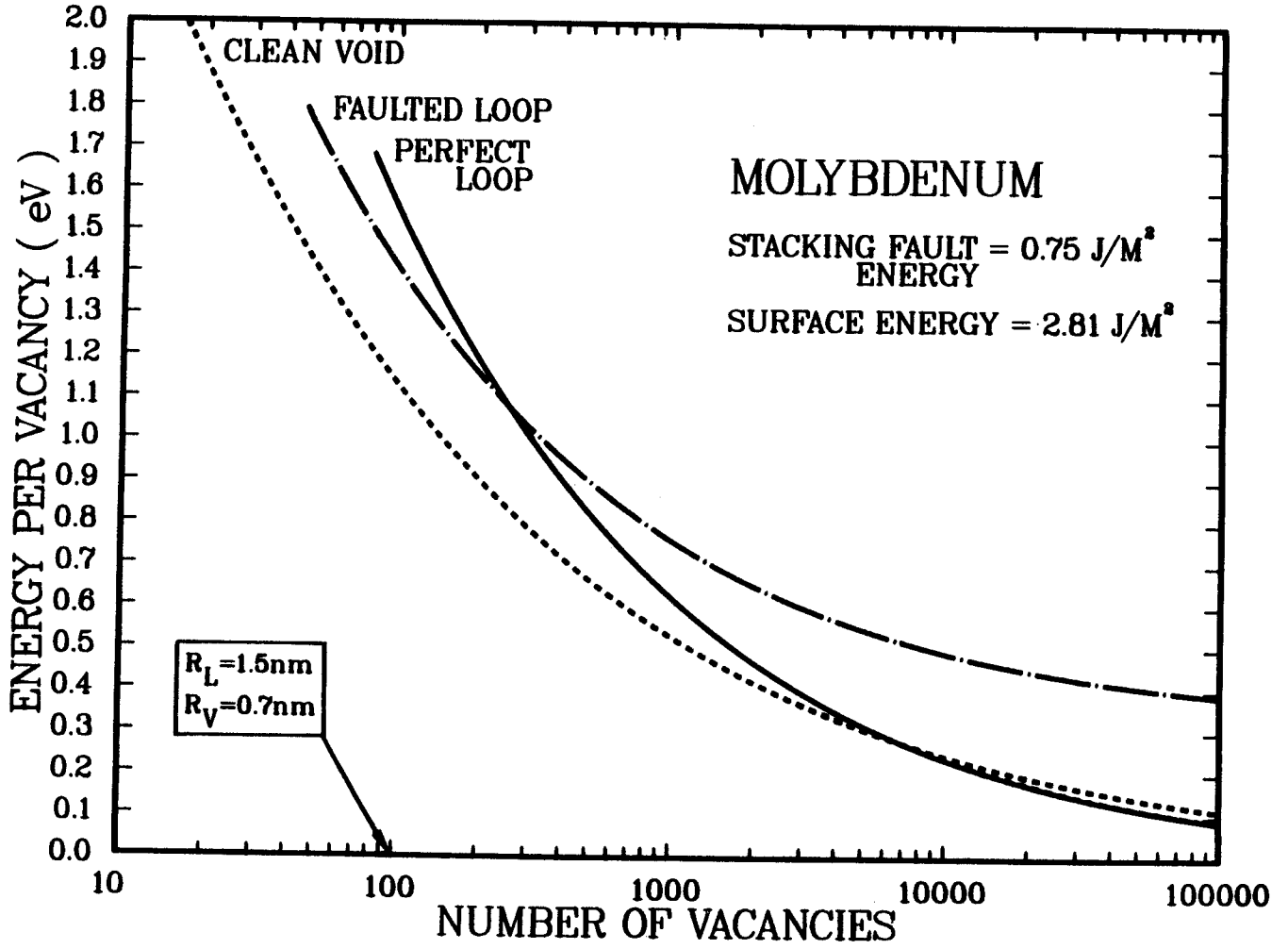

Figure 8. Calculated specific energies of vacancy clusters in pure molybdenum.